IEEE Photonics Journal
An IEEE Photonics Society Publication

Open Access

A Novel Iterative-SLM Algorithm for PAPR Reduction in 5G Mobile Fronthaul Architecture

Volume 11, Number 1, February 2019

Mohammed I. Al-Rayif
Hussein Seleem
Amr Ragheb
Saleh Alshebeili

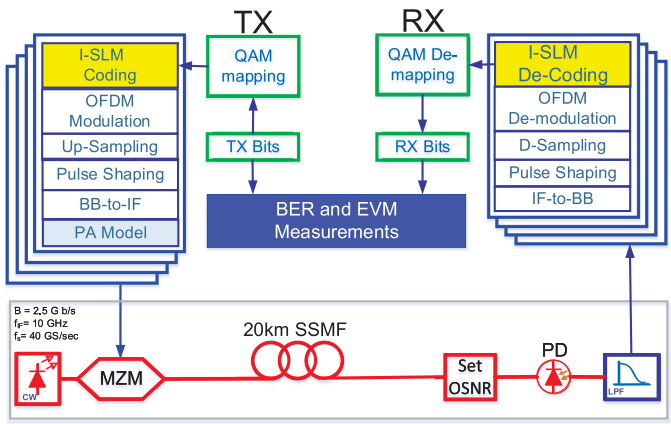

DOI: 10.1109/JPHOT.2019.2894986
1943-0655 © 2019 IEEE

IEEE photonics SOCIETY

IEEE

A Novel Iterative-SLM Algorithm for PAPR Reduction in 5G Mobile Fronthaul Architecture

Mohammed I. Al-Rayif,[1,2] Hussein Seleem [3], Amr Ragheb [4], and Saleh Alshebeili[4]

[1]Department of Electrical Engineering, Al-muzahmia Branch, King Saud University, Riyadh 12372, Saudi Arabia
[2]College of Engineering, King Khalid University, Abha 61421, Saudi Arabia
[3]Department of Electronics and Electrical Communications, Faculty of Engineering, Tanta University, Tanta 3111, Egypt
[4]KACST-TIC in Radio frequency and Photonics for the e-Society, Department of Electrical Engineering, King Saud University, Riyadh 11421, Saudi Arabia

DOI:10.1109/JPHOT.2019.2894986

Manuscript received December 4, 2018; revised January 14, 2019; accepted January 21, 2019. Date of publication January 23, 2019; date of current version February 8, 2019. This work was supported by King Saud University, Deanship of Scientific Research under Grant NFG-7-18-03-15. Corresponding author: Hussein Seleem (e-mail: eltaibee@f-eng.tanta.edu.eg).

Abstract: One of the main drawbacks of orthogonal frequency division multiplexing (OFDM) is the unpredictable significant increase in the peak-to-average power ratio (PAPR), due to the large dynamic range of the OFDM symbol waveforms. To overcome this problem, we propose a novel PAPR reduction technique in the transmitter DSP of a fiber mobile fronthaul network, named as iterative selective mapping (I-SLM). The proposed algorithm uses orthogonal phase vectors construction. Several alternative sets of the OFDM symbol are iteratively generated by deterministic sets of orthogonal phase vectors and the one which introduces the lowest peak power value is considered for transmission. Simulation results demonstrate a substantial PAPR reduction, comparing to the partial orthogonal selective mapping (POSLM), especially when the number of iterations increases in the presence of different variables, such as the number of OFDM subcarriers/frame and the modulation order.

Index Terms: Peak-to-average power ratio (PAPR), non-linear power amplifier, VPItransmissionMaker, partial orthogonal selective mapping (POSLM), complementary cumulative distribution function (CCDF).

1. Introduction

The surge increase in data traffic, generated by various interactive services, demands a dense deployment of small cell antenna sites and higher channel bandwidth. Recently, millimeter wave (MMW) frequencies in conjunction with a centralized radio access network (C-RAN) architecture is introduced as a smart solution for high capacity applications and better coordination among cells. In C-RAN architecture, the functionalities of the traditional base stations (BSs) are split between the baseband unit (BBU) and remote radio head (RRH) unit. The centralized BBU performs the baseband processing of multiple BBUs at a common location, while simpler RRH units perform the radio processing, with low energy consumption, at the antenna site. This requires both BBU

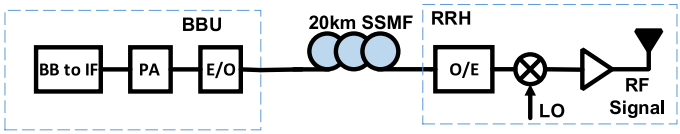

Fig. 1. A simplified block diagram of an analog IF over fiber (IFoF) in a downlink transmission.

and RRH units to be connected through a high speed, low latency and accurately synchronized network, referred to as the mobile fronthaul [1].

Recently, fiber technologies have been extensively exploited in demonstrating next generation wireless networks i.e. 5G, MMW generation, and internet of things (IoT). This is due to the capabilities of photonics technology such as low power loss, high speed, low latency, and immunity to electromagnetic (EM) interference. The wireless signals can be transmitted through the fronthaul network in analog or digital domain at baseband or passband with respect to an optical carrier, resulting in different fronthaul schemes [1], [2]. For instance, digitized baseband signal over fiber based common public radio interface (CPRI) mobile fronthaul scheme requires 32 Gb/s optical line rate for serving a four sector 8×8 MIMO antenna site for 20 MHz bandwidth wireless channel [3]. CPRI fronthauling architecture is more inefficient and complex for providing multiple services through the same fiber. Analog RF signals over fiber schemes increase the bandwidth efficiency and reduce the latency by avoiding the use of expensive A/D and D/A converters at the RRH for the digitization process, as required by CPRI [1]. However, it requires optical components that work at bandwidths of at least the RF carrier frequencies. On the other hand, analog RF signals at IF over fiber provides more flexibility and uses lower bandwidth optical components compared to RF and millimeter wave signal over fiber network, required for 5G signals fronthauling [4]. A simplified schematic diagram of an analog IF over fiber scheme for a downlink scenario is shown in Fig. 1, where the baseband signal is converted to IF frequencies in the centralized BBU before transmission through fiber, which is further up-converted to the desired RF signal at the RRH.

On the other side, orthogonal frequency division multiplexing (OFDM) waveforms have been adopted in the majority of wireless systems and recently in short and long reach optical communications, due to its high spectral efficiency and robustness to channel impairments in both wireless and optical systems. However, the digital implementation of OFDM using the fast Fourier transform (FFT)/inverse fast Fourier transform (IFFT) generates high peaks in the obtained OFDM signals, known as high peak to average power ratio (PAPR). This produces a distorted OFDM signals due to the clipping of the non-linear transmission components/devices. In optical OFDM (O-OFDM) system, this arises from various nonlinear elements such as the digital-to-analog converter (DAC), the electrical power amplifier (PA), and the optical modulator [5]–[10]. Thus, a PAPR reduction technique is needed as another option to cope with this phenomenon. In this regards, different techniques and algorithms have been proposed in the literature, for instance, clipping and filtering [9], block-coding [10], probabilistic methods [7], [8], [11], [12], and discrete-Fourier-transform spread (DFT-spread) in the IM/DD system [13]. All these attractive methods participate in reducing the PAPR but at the expense of, in somehow, system's performance, efficiency, or complexity.

In this work, we propose a PAPR reduction scheme that mitigates the effect of PA in O-OFDM systems. This is classified as a distortion-less scheme as it depends on a deterministic orthogonal phase vectors for PAPR reduction which does not destroy the original phases sequence, as in selective mapping (SLM) and partial transmit sequence (PTS) schemes [14]. Moreover, we consider the partial orthogonal-selective mapping (POSLM) in this work here for comparison purposes. Recently, a huge number of research related to these schemes have been conducted. The conventional SLM and PTS depend on a random candidates phase vectors U, to shift the original OFDM data phases randomly in order to reduce its PAPR. It is worthy to note that a transmission of side information is required to identify the index of the applied phase vector at the transmitter, which introduces a low system efficiency [15]. The side information constraint has been subjected to exclusion from transmission by a number of demonstrations, for instance, in [7], [12], the uncorrelated elements

inside the candidate phase vector are extended to a specific value in order to increase the system spectral efficiency. Note that a full operation power for recovery is needed at the receiver side to identify the considered transmitted phase vector. This results in high computational complexity [11], [16].

Recently in [8], [17], The authors discussed the trade off between the system bit error rate (BER) and PAPR performances in conjunction with its computational complexity. Briefly, in [8], a semi-blind selected mapping scheme is addressed for PAPR reduction. Though, such a scheme enables both low computational complexity and embedding of the side information into the pilot sub-carriers at the transmitter, the provided BER performance in the code of suboptimal recovery is incomparable with that of the decoded SLM technique. Besdies, the PAPR reduction in [18] with the Class-III SLM scheme still needs to transmit $\lceil \log_2 U \rceil$ side information bits, where U is the number of phase vectors, i.e. low system efficiency. Additionally, a PAPR reduction technique using biased subcarriers has been investigated in [19], where a comparable PAPR characteristic has been obtained at high values of real δ_r and imaginary δ_i components of the time domain reference sample. However, at a reasonable values of those components (i.e. smaller values), for example: $\delta_r = \delta_i = 0.75$, the complementary cumulative distribution function (CCDF) PAPR curves become worse. In [20] the authors suggested a cyclic shifted sequences (CSS) scheme which is evolved from the PTS scheme to improve the PAPR reduction performance. It can be noticed that an extra computational complexity is introduced when implementing the IFFT for the PTS and CSS schemes. Finally, in [17], a low complexity PTS scheme using dominant time domain samples in OFDM systems has been demonstrated.

In this work, we successfully demonstrate the transmission of 4G-LTE analog IF signal over 20 km fiber fronthaul link that feeds data to a heterogeneous RRH site. VPItransmissionMaker ver 9.9 [21] is used to build and model the whole transmission system. Particularly, a deterministic phase vectors sets based on Hadamard orthogonal matrix are built intelligently such that for each iteration, a specific phase vectors design is applied in order to reduce the correlation with the previous iteration. As a result, this method shows an acceptable performance in terms of PAPR, BER and error vector magnitude (EVM) at different OSNR values.

The rest of the paper is organized as follows; a description of the proposed I-SLM scheme is given in Section-2. Section-3 presents the system model of the proposed I-SLM scheme. Simulation and analytical results are presented and discussed in Section-4. Finally, Section-5 provides concluding remarks.

2. The Proposed Iterative- SLM (I-SLM) PAPR Reduction Scheme

In this section the proposed algorithm will be briefly discussed. Let

$$\mathbf{X} = [X(0), X(1), \ldots, X(k), \ldots, X(K-1)]$$

denotes an input symbol sequence to the IFFT which consists of K complex transmitted data, where $0 \leq k \leq K-1$. Such a symbol sequence has an L-ary quadrature amplitude modulation (QAM), and the IFFT output symbol sequence $\mathbf{x} = [x(0), x(1), \ldots, x(n), \ldots, x(K-1)]$ is formed with K subcarriers, where $0 \leq n \leq K-1$. As mentioned in the previous section, OFDM system leads to an arbitrary high peak subcarrier, the thing which makes the peak reduction technique essential. Consequently, in this paper, the input phases sequence are iteratively generated though a number of phase blocks to satisfy the required PAPR reduction, instead of treating this matter via a fixed number of phase blocks as the conventional SLM and PTS methods. Hereafter, to perform the library of the iterative (candidates) phase vectors, as depicted in Fig. 2, an orthogonal Hadamard $Q \times Q$ matrix with $Q = 2^i$ and $i \geq 1$ can be expressed as

$$\mathbf{S} = \begin{bmatrix} s_{11} & \cdots & s_{1Q} \\ \vdots & \ddots & \vdots \\ s_{Q1} & \cdots & s_{QQ} \end{bmatrix}, \tag{1}$$

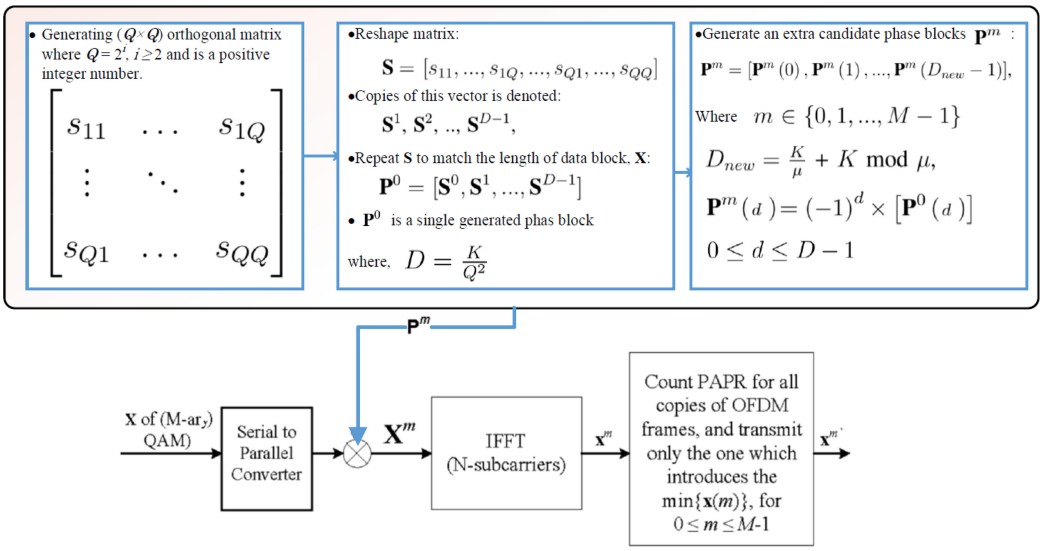

Fig. 2. Process of generating the library of the candidate phase vectors.

TABLE 1

An Example of the I-SLM Scheme to Generate Three Phase Vectors With $K = 8$ Elements per Phase Vector and Two Iterations at Different Number of Sub-Vectors $\mu = 2$ and 4, Where $\mathbf{P}^0$ Os Constructed From (2×2) Orthogonal Hadamard Matrix, and $\mathbf{P}^m = (-1)^d \times [\mathbf{P}^0(n_d)]$ With $m = 1, 2$ According to the Distribution of d, (Note That; in This Example, $K \bmod \mu = 0$)

	n	0	1	2	3	4	5	6	7
	$\mathbf{P}^0$	1	1	1	-1	1	1	1	-1
Iteration-1: $\mu = 2$, $\mathbf{P}^1 = (-1)^{d_1} \times \mathbf{P}^0(n_{d_1})$	d_1	1		2		3		4	
	$\mathbf{P}^1$	-1	-1	1	-1	-1	-1	1	-1
		$(-1)^{d_1} \times [p_0^0, p_1^0]$		$(-1)^{d_1} \times [p_2^0, p_3^0]$		$(-1)^{d_1} \times [p_4^0, p_5^0]$		$(-1)^{d_1} \times [p_6^0, p_7^0]$	
Iteration-2: $\mu = 4$, $\mathbf{P}^2 = (-1)^{d_2} \times \mathbf{P}^0(n_{d_2})$	d_2	1				2			
	$\mathbf{P}^2$	-1	-1	-1	1	1	1	1	-1
		$(-1)^{d_2} \times [p_0^0 ... p_3^0]$				$(-1)^{d_2} \times [p_4^0 ... p_7^0]$			

where $\{s\}_{rc} \in \{-1, +1\}$ and $1 \leq r, c \leq Q$. and $Q << K$. Next, this small size matrix $\mathbf{S}$ is reorganized to obtain the first phase vector $\mathbf{P}^0$. Therefore, the matrix $\mathbf{S}$ is reshaped to produce the vector $\mathbf{S}^0$ of dimension $(1, Q \times Q)$, i.e. $\mathbf{S}^0 = [s_{11}, \ldots, s_{1Q}, \ldots, s_{Q1}, \ldots, s_{QQ}]$. Copies of this vector, denoted by $\mathbf{S}^1$, $\mathbf{S}^2$, .., $\mathbf{S}^{D-1}$, are then concatenated to obtain the first phase vector $\mathbf{P}^0 = [\mathbf{S}^0, \mathbf{S}^1, \ldots, \mathbf{S}^{D-1}]$, to match the length of data block K, where $0 \leq d \leq D-1$ and $D = \frac{K}{Q^2}$ is the number of sub-vectors (groups) per the vector $\mathbf{P}^0$.

For the next iteration, to construct a modified phase vector, a new number of sub-vectors D is generated, i.e. $D_{new} = \frac{K}{\mu} + K \bmod \mu$, where μ is any arbitrary positive integer number. In this formulation, the factor μ is varied from 1 to M, where M is the maximum number of iterations. Particularly, each value of μ indicates the length of a subvector per a single phase vector. Therefore, a new candidate phase vector $\mathbf{P}^m$ is generated based on the phase vector $\mathbf{P}^0$. such that $\mathbf{P}^m = [\mathbf{P}^m(0), \mathbf{P}^m(1), \ldots, \mathbf{P}^m(D_{new}-1)]$, where $\mathbf{P}^m(d) = (-1)^d [\mathbf{P}^0(d)]$ is the d^{th} updated sub-vector for the m^{th} phase vector, $\forall d \in \{0, 1, \ldots, D_{new}-1\}$ and $m \in \{0, 1, \ldots, M-1\}$. It is clear that all iterated phase vectors are not random, but depend on the root phase vector $\mathbf{P}^0$ whose elements (and subvectors) are constructed orthogonally, see the example illustrated in Table 1.

Without loss of generality, the produced phase vectors M are multiplied by the corresponding input data sequence, element by element, prior to the OFDM system to obtain $M-$ copies of the output symbol sequence $\mathbf{x} = [\mathbf{x}^0, \mathbf{x}^1, \ldots, \mathbf{x}^{M-1}]$, where $\mathbf{x}^m = IFFT\{\mathbf{X}\mathbf{P}^m\} = [x_0^m, x_1^m, \ldots, x_{K-1}^m]$. The

Algorithm 1: Intelligent Iterative PAPR Reduction Scheme.

Input: $\mathbf{x}_0$, $\mathbf{x}_{org}$
Initialize: $\text{PAPR}_{intial} = \left[\text{PAPR}_0, \text{PAPR}_{org}\right]$
$\mathbf{x}_{intial} = [\mathbf{x}_0, \mathbf{x}_{org}]$
for $m = 1 : M$ - the number of iterations **do**
  $[\text{PAPR}_{min}, \text{INDEX}_{min}] = \min(\text{PAPR}_{intial})$
  $\mathbf{x}_{new} = IFFT[\mathbf{x}_m] \longrightarrow \text{PAPR}_{new} =$ **function** $\{\textbf{PAPR}\,[\mathbf{x}_{new}]\}$
  if $\text{PAPR}_{new} < \text{PAPR}_{min}$ **then**
    $\mathbf{x}_{intial}(\text{INDEX}_{min}) = \mathbf{x}_{new}$
    $\text{PAPR}_{intial}(\text{INDEX}_{min}) = \text{PAPR}_{min}$
  end if
end for
Output: $\mathbf{x}_{new}$, PAPR_{min}

PAPR is determined for each m consequential OFDM symbol as follows

$$PAPR_m = \frac{\max_n \left[\left|x_n^m\right|^2\right]}{E\left[\left|x_n^m\right|^2\right]} = \frac{\max_n \left[\left|x_n^m\right|^2\right]}{\sigma_x^2}, \qquad 0 \le m \le M-1. \tag{2}$$

The m^{th} OFDM symbol with the lowest PAPR, $x^{\acute{m}}$, is considered for transmission, that is ;

$$\mathbf{x}^{m'} = \mathbf{x}^m \left\{ \arg\min_{0 \le m \le M-1} [PAPR_m] \right\}. \tag{3}$$

To guarantee achievement of optimal PAPR reduction for the given OFDM symbol, the original PAPR is compared with the first iterated OFDM-PAPR frame P^0. Next, only the minimum one is considered for further process of comparisons with the next iterations of OFDM-PAPR(s), as illustrated in Algorithm-1.

To conclude, the characteristic of the proposed PAPR reduction is evaluated by figuring out the complementary commutative-distribution function (CCDF) of the lowest obtained $PAPR_{m'}$ for an OFDM frame. Theoretically, the CCDF of the $PAPR_{m'}$ is defined as the probability that the lowest $PAPR_{m'}$ exceeds a given threshold $PAPR_0$ as following [22]:

$$Pr\{PAPR_{m'} > PAPR_0\} = \left(1 - \left(1 - e^{-PAPR_0}\right)^K\right)^M, \tag{4}$$

where M is the maximum number of iterations. However, such a formula does not consider the effect of the extension factor, which is applied in our work for recovery stage in the receiver side. Therefore, equation (4) is approximated to the formula expressed in (5) when presuming the presence of extension factor C, as follows:

$$Pr\{PAPR_m > PAPR_0\} = \left(1 - \left(1 - e^{-PAPR_0 - \log_{10} C}\right)^K\right)^M, \tag{5}$$

where $C = 1 + |\epsilon|$ and $|\epsilon| \in \{\mathbb{Q}\}$ indicate the fraction extended amount. In brief, this modified value of the threshold is derived based on extensive simulation results, considering the increase in average energy per complex symbol, along the lines of deriving the theoretical CCDF-PAPR of I-SLM.

To recover the original phase sequences at the receiver, the received data frame which contains the m'_{th} phase vector, y_{in}, should be restored back to the original phases; that is, we remove the effect of the m'_{th} vector from the received signal, with no side information for recovery purpose was transmitted. Therefore, the concept of extended specific elements [12] is implemented on the candidate phase vector m' at the transmitter side as described in the following example. Consider four phase vectors were generated with length of $K = 8$ for each, i.e. $M = 4$ iterations, hence $\alpha = \frac{K}{M} = 2$ elements will be extended to the value C per phase vector. In order to guarantee a

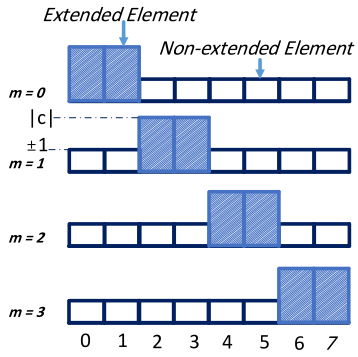

Fig. 3. An example of the conceptual extended candidate vectors.

non-correlated extension between the M-phase vectors, the extension elements are shifted with respect to the increase of m, $m = 0, 1, 2, 3$. In other words, for $m = 0$, the first and second elements are extended to C-value, while as at $m = 1$, the third and forth elements are extended and so on; see Fig. 3.

Hereafter, at the receiver, the formula of [12], is implemented in this study as follows:

$$P^{m'} = \underset{\substack{0\le m\le M-1\\ 0\le n\le K-1}}{\operatorname{argmin}} \left| |Y(n)|^2 - |H(n)|^2\sigma_x^2|P^m(n)|^2 - \sigma_n^2 \right| \tag{6}$$

where $P^{m'}$ indicates the estimated (desired) phase vector, $Y = FFT(y)$ is referred to as the received sample. $H = FFT(h)$ is the multipath fading channels, σ_n^2 : denotes the power spectral density of AWGN channel. σ_x^2 : is the average energy per complex symbol of L-QAM, $P_m(n)$: is the m^{th} tested phase vector, $0 \le m \le M-1$, and $|.|$ is the modulus operation. It is worth mentioning that the quantity $|H(n)|^2$ is set to 1 in the case of considering AWGN channel and flat optical channel, as demonstrated in the following sections.

We believe that our proposed I-SLM differs from the other recent techniques such as POSLM and conventional PTS from two points of view. The first is that the construction of each generated phase vector of I-SLM depends on deterministic sequences, which will be helpful, as a future work, to recover the desired phase vector blindly. Secondly, from the BER/EVM performance view point, it is noticeable that the proposal outperforms the others, in both scenarios; the wireless and the optical communication systems.

3. Numerical Results and Discussions

The VPItransmissionmaker simulation setup is shown in Fig. 4. An intensity modulation-direct detection (IM-DD) link is built to verify the feasibility of the proposed scheme for mobile fronthaul PAPR reduction. In the TX side, the generated pseudo-random binary sequence (PRBS) are mapped into QAM symboles through a QAM coder module, then they are pre-coded using the proposed PAPR reduction algorithm. Next, they go into subcarrier mapping and OFDM modulation modules. After up-sampling and conversion to IF, the IF signal is converted to optical signal by a Mach-Zehnder modulator (MZM) with a continuous wave laser. Finally, after 20 km standard single mode fiber (SSMF), the signal is detected and sampled in the RRH unit. Typically, in RRH's DSP, the samples are converted from IF to radio frequencies (RF). But in our demonstration, the IF signal is converted to baseband signal to study our proposed scheme then the OFDM streams are demodulated through time synchronization for each frame, cyclic prefix (CP) removal, frequency synchronization, FFT and QAM demodulation.

In this section, the performance characteristics of the proposed I-SLM scheme in terms of PAPR reduction, power spectral density (PSD), BER and error vector magnitude (EVM) are numerically

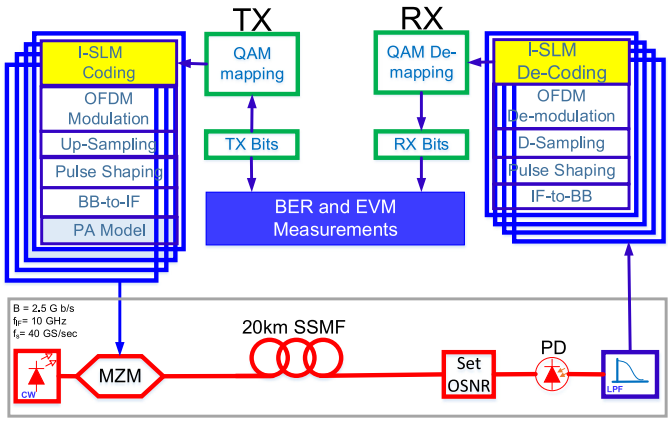

Fig. 4. A Model for optical system with an iterative OFDM-PAPR reduction.

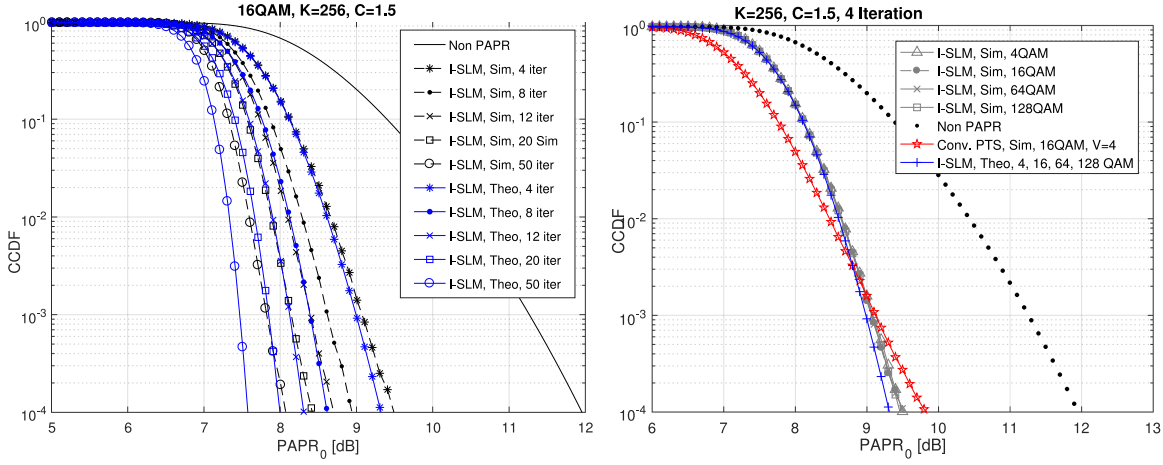

(a) Various number of iterations (b) Various QAM orders

Fig. 5. CCDF of the proposed OFDM-PAPR reduction algorithm.

investigated for various parameters such as extension value C, OFDM block length K, and the size of QAM constellation. For comparison purposes, the techniques POSLM [16], [23] and conventional-PTS [17] have been considered in this section. Also, the conventional-SLM is not represented here because the POSLM provides a sufficient discussion, however for further information see [12], [14], [16], [18]. It is worth to mention that the computation cost of the POSLM and the proposed I-SLM is presented in Table 1, in terms of the complex multiplications and the complex additions, where N is the number of subcarriers, U is the number of phase vectors, and M is number of iterations.

3.1 Complementary Cumulative Distribution Function (CCDF)

The CCDF of the PAPR reduction is used to evaluate the characteristics for the proposed I-SLM scheme in addition to the POSLM and conventional PTS schemes for comparisons purposes, as illustrated in Figs. 5 and 6.

As shown in Fig. 5a, various iteration values are demonstrated with 16QAM, 256 FFT size and extended value $C = 1.5$. It is clear that the proposed scheme helps to reduce the high arbitrary peaks. It can be noticed that, when the number of iteration increases, the CCDF improves but with an increment in the computational complexity as well as presented in table 2. Moreover, increasing

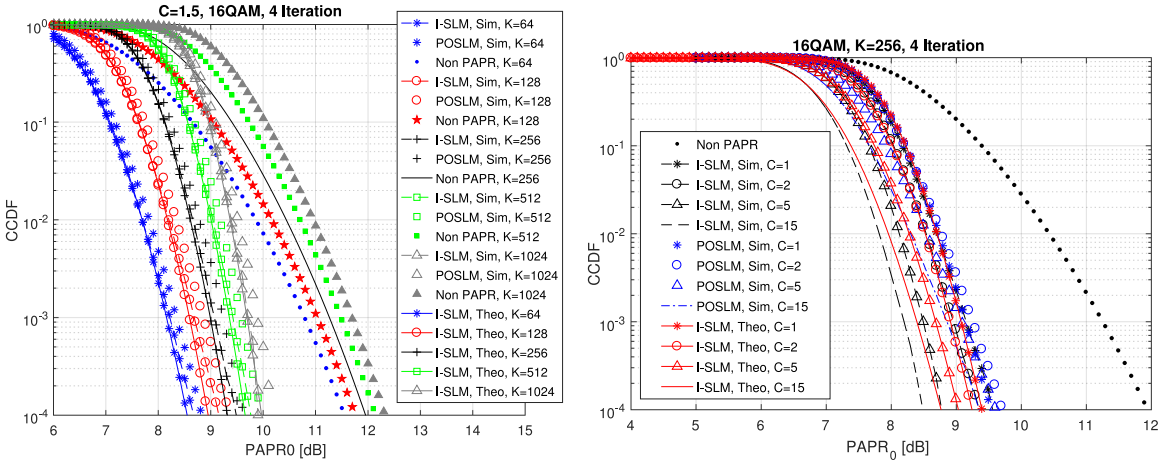

(a) Various FFT size values (b) Various extension factor values

Fig. 6. CCDF of the I-SLM and POSLM OFDM-PAPR reduction algorithms.

TABLE 2
Computational Complexity of Conventional SLM, POSLM, and Proposed I-SLM Schemes

	Number of Complex Multiplications	Number of Complex Additions
POSLM	$UN/2\log_2 N + (N/2)^2U$	$UN\log_2 N + (N/2)(U+1) - U$
I-SLM	$MN/2\log_2 N + N^2(M+3)$	$MN\log_2 N + 2(N-1)M$

the QAM order has no tangible change in the CCDF at a certain iteration value, as illustrated in Fig. 5 b, for $K = 256$ subcarriers, $C = 1.5$ and $M = 4$ iterations. In this figure, the performance of conventional PTS is presented against our proposed scheme where we observe the superiority of the later. It is worth mentioning that in Fig. 5 b, all comparisons have been tested such that the number of generated phase vectors U in POSLM, sub-block phase vectors in conventional PTS, and number of iterations in proposed I-SLM are assumed equal to achieve a fair comparison.

In addition, Fig. 6 represents the CCDF-PAPR of the proposed I-SLM at different values of K subcarriers (Fig. 6a), and C extension factor (Fig. 6b). The results are compared with those of the POSLM scheme. Generally, from Fig. 6a, all performances become worse when increasing the length of the transmitted frame, where the probability of obtaining high PAPR will be elevated, and vise versa in case of low value of K representing number of subcarriers. It is worth to note that for all values of K, the proposed I-SLM preforms better than POSLM. Furthermore, Fig. 6b indicates the superiority of the proposed I-SLM over the POSLM scheme, when the value of C is increased gradually. Though such large values of C can not be applied in practice, causing a negative impact on the performance of the system in terms of BER/EVM [23], however it is illustrated here just to study the behavior of the system to determine the influences of all factors.

Modeling the nonlinear response of PAs can take many forms. In this work, we use the solid state power amplifier (SSPA) model developed in [5], [24]. In the SSPA model, The gain $g_{SSPA}(P_{in})$ can be written as:

$$g_{SSPA}(P_{in}) = \frac{g_0\sqrt{P_{sat}}}{\left[1 + (\frac{P_{in}}{P_{sat}})^r\right]^{\frac{1}{2r}}} \tag{7}$$

where g_0 is the small signal gain, r adjusts AM/AM saturation sharpness, P_{in} is the input power and P_{sat} is the saturation power. In order to quantify nonlinear distortion induced by PA, we define input

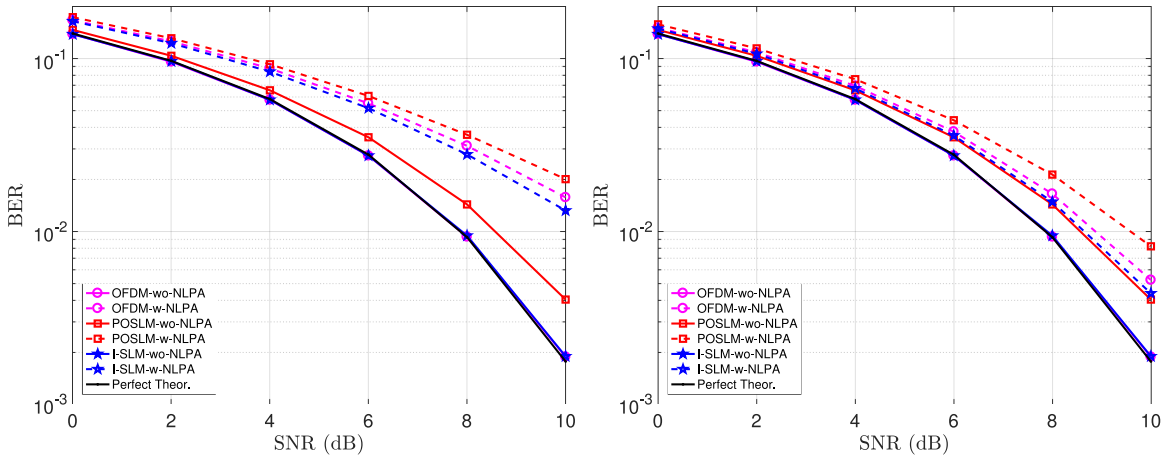

(a) $IBO = 3$ (b) $IBO = 5$

Fig. 7. BER versus SNR for original OFDM, POSLM and the proposed iterative OFDM-PAPR reduction with/without nonlinear PA with $r = 3$, $C = 1.5$, $K = 256$ subcarriers, and assuming AWGN channel.

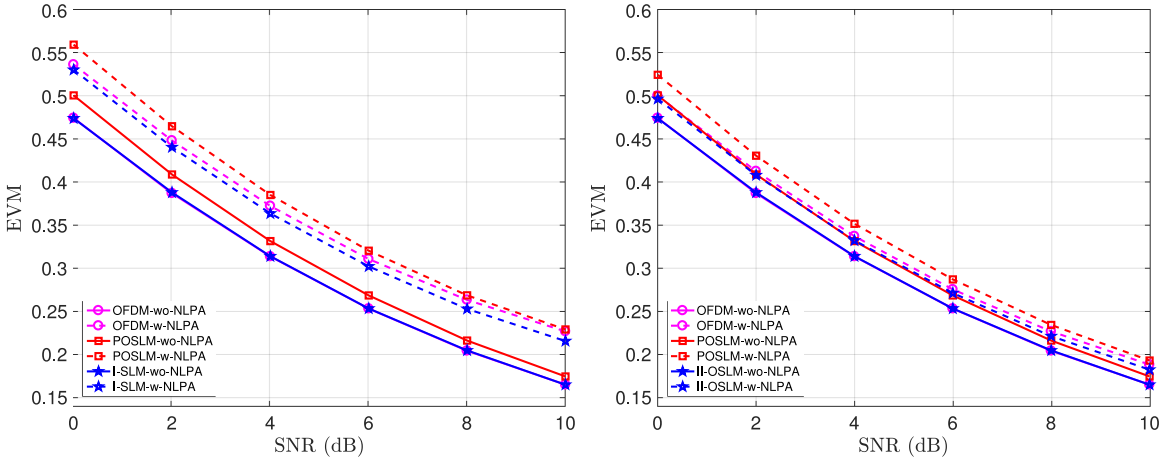

(a) $IBO = 3$ (b) $IBO = 5$

Fig. 8. EVM versus SNR for original OFDM, POSLM and proposed I-SLM with/without nonlinear PA with $r = 3$, $C = 1.5$, $K = 256$ subcarriers, and assuming AWGN channel.

backoff (IBO) as the ratio between input saturation and average power, i.e., $IBO = \frac{P_{sat}}{P_{avg}}$. While higher IBO gives a more linear response, it leads to an inefficient PA. High bandwidth communications systems require significant trade-off between efficiency and distortion, as wideband linear amplifiers significantly increase the system cost.

3.2 Bit Error Rate (BER) Performance

The BER performance of the conventional OFDM, POSLM, and proposed I-SLM schemes are tested with/without a nonlinear solid state power amplifier (SSPA) model [5], [24] in VPItransmissionmaker package assuming AWGN channel, wireless fading channel and optical channel for back-to-back (B2B) and 20 km fiber length as shown in Figs. 7–10, respectively. In Fig. 7 and 8, different input back-off (IBO) values of the nonlinear amplifier are assumed, (a) $IBO = 3$ and (b) $IBO = 5$ dB, for $K = 256$ subcarriers and with extension factor $C = 1.5$.

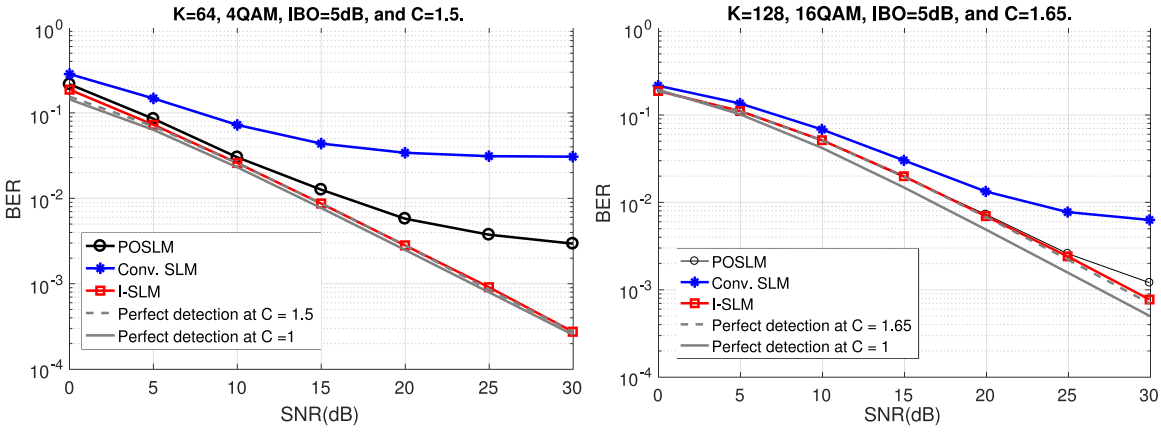

(a) $K = 64$ subcarriers and $C = 1.5$ (b) $K = 128$ subcarriers and $C = 1.65$

Fig. 9. BER versus SNR for POSLM, conventional SLM and the proposed I-SLM with nonlinear PA with $r = 3$, $IBO = 5$, and assuming wireless fading channel with number of paths $L = K/8$.

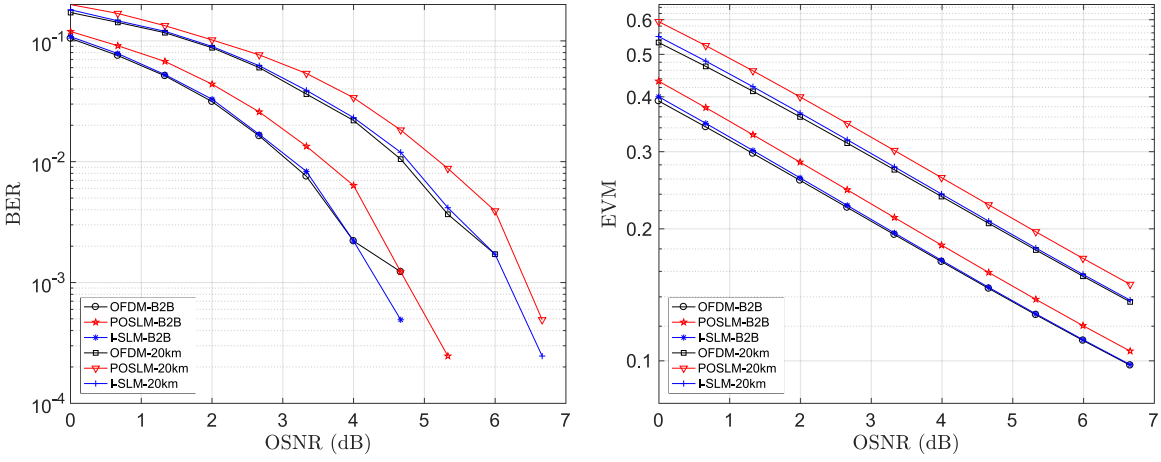

(a) BER versus OSNR (dB) (b) EVM versus OSNR (dB)

Fig. 10. (a) BER and (b) EVM versus OSNR for non-PAPR reduction, POSLM and proposed iterative OFDM-PAPR reduction where $C = 1.5$, $K = 256$ subcarriers, assuming optical link.

The simulation results show that the proposed scheme outperforms other techniques with/without the nonlinear power amplifier. As the value of IBO increases, all performances improve but our proposed scheme remains the best. Additionally, if the extension factor is extended a bit more, say $C = 1.7$, the performance of the proposed technique will even perform better, but this action could lead to higher power consumption.

From Fig. 9, it can be illustrated that the performance of the proposed I-SLM is better than others, in presence of fading wireless channel and the power amplifier. Beside that, the difficulty of a low IBO can be overcome by increasing a fractional value to the extension factor C, as can be demonstrated in the Fig. 9 b. Also, in this figure, a small gap (about 1dB) is observed between the performance of theoretical curves at C = 1 and C = 1.65, which probably due to the increase in the extension value, that is the fraction $10\log(0.65)$ dB.

Fig. 10 depicts the (a) BER (b) EVM performances versus OSNR for non-PAPR reduction case, POSLM scheme, and the proposed I-SLM technique, with/without nonlinear power amplifier, at $r = 3$, $IBO = 5$, $C = 1.5$, and $K = 256$ subcarriers, and assuming optical link with both back-to-

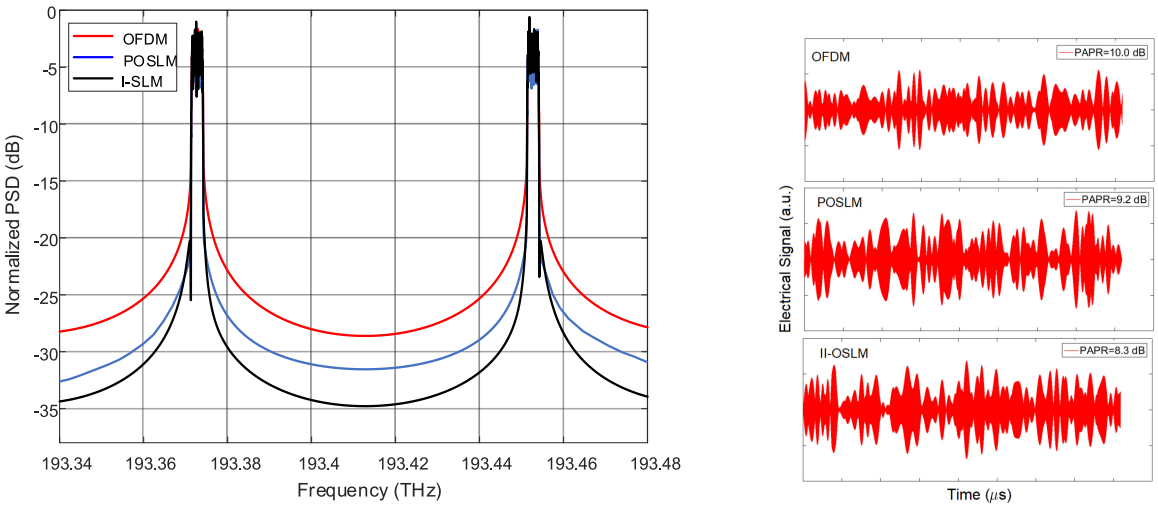

(a) Frequency domain (b) Time domain

Fig. 11. (a) PSD and (b) time domain representation of conventional OFDM, POSLM OFDM, and I-SLM OFDM.

back and 20 km fiber length. Thanks to the proposed I-SLM, the performances of the system (in both cases, B2B and 20 km length) are almost identical to the original OFDM performances of both scenarios, while it is outperforms the POSLM scheme.

3.3 Power Spectral Density (PSD) Performance

In this section, we study the behavior of the proposed technique (I-SLM) from the point of view of PSD in comparison with the POSLM and the conventional OFDM signals, as shown in Fig. 11 in (a) frequency domain and (b) time domain. The proposed I-SLM scheme introduces an improvement in the out-of-band radiation while reducing its PAPR compared to the situation of POSLM and that of the conventional OFDM, used here as a benchmark for comparison. For example, at the frequency 193.415 THz, it is observed that the proposed scheme gains about 4 dB over the POSLM, where 2 dB approximately of PAPR is reduced from the original OFDM sample.

4. Conclusion

In this paper, an intelligent iterative PAPR reduction method is proposed. It depends on a generated set of orthogonal phase vectors which are iteratively constructed in a deterministic form based on the Hadamard orthogonal matrix. The algorithm is referred to as iterative SLM (I-SLM). The performance of this technique is represented at different constellation sizes, K subcarriers, C extension factors, and M number of iterations. The results of the proposed I-SLM provides superior results for the cases of AWGN channel and optical fiber channels with B2B and 20km fiber length. The PAPR can be reduced about 3dB from the original OFDM curve at $K = 256$ subcarriers, 16 QAM, and C=1.5. Also, I-SLM gains about 0.5dB over POSLM when implemented in optical systems, whereas it performs similar to conventional OFDM.

References

[1] C. Lim *et al.*, "Fiber-wireless networks and subsystem technologies," *J. Lightw. Technol.*, vol. 28, no. 4, pp. 390–405, Feb. 2010.
[2] T. Pfeiffer, "Next generation mobile fronthaul architectures," in *Proc. Opt. Fiber Commun. Conf.*, 2015, Paper M2J–7.

[3] A. de la Oliva, J. A. Hernández, D. Larrabeiti, and A. Azcorra, "An overview of the CPRI specification and its application to C-RAN-based LTE scenarios," *IEEE Commun. Mag.*, vol. 54, no. 2, pp. 152–159, Feb. 2016.
[4] P. T. Dat, A. Kanno, N. Yamamoto, and T. Kawanishi, "5G transport networks: The need for new technologies and standards," *IEEE Commun. Mag.*, vol. 54, no. 9, pp. 18–26, Sep. 2016.
[5] S. Amiralizadeh, A. T. Nguyen, and L. A. Rusch, "Modeling and compensation of transmitter nonlinearity in coherent optical OFDM," *Opt. Exp.*, vol. 23, no. 20, pp. 26192–26207, 2015.
[6] S. Amiralizadeh and L. Rusch, "Transmitter sensitivity to high PAPR in coherent optical OFDM systems," in *Proc. CLEO: Science Innovations.*, 2014, Paper SW1J–5.
[7] N. Chen and G. T. Zhou, "Peak-to-average power ratio reduction in OFDM with blind selected pilot tone modulation," *IEEE Trans. Wireless Commun.*, vol. 5, no. 8, pp. 2210–2216, Aug. 2006.
[8] J. Ji, G. Ren, and H. Zhang, "A semi-blind SLM scheme for PAPR reduction in OFDM systems with low-complexity transceiver," *IEEE Trans. Veh. Technol.*, vol. 64, no. 6, pp. 2698–2703, Jun. 2015.
[9] K. Anoh, C. Tanriover, and B. Adebisi, "On the optimization of iterative clipping and filtering for PAPR reduction in OFDM systems," *IEEE Access*, vol. 5, pp. 12004–12013, 2017.
[10] R. Yoshizawa and H. Ochiai, "Energy efficiency improvement of coded OFDM systems based on PAPR reduction," *IEEE Syst. J.*, vol. 11, no. 2, pp. 717–728, Jun. 2017.
[11] H.-S. Joo, S.-J. Heo, H.-B. Jeon, J.-S. No, and D.-J. Shin, "A new blind SLM scheme with low decoding complexity for OFDM systems," *IEEE Trans. Broadcast.*, vol. 58, no. 4, pp. 669–676, Dec. 2012.
[12] S. Y. Le Goff, S. S. Al-Samahi, B. K. Khoo, C. C. Tsimenidis, and B. S. Sharif, "Selected mapping without side information for PAPR reduction in OFDM," *IEEE Trans. Wireless Commun.*, vol. 8, no. 7, pp. 3320–3325, Jul. 2009.
[13] F. Li, X. Li, J. Zhang, and J. Yu, "Transmission of 100-Gb/s VSB DFT-spread DMT signal in short-reach optical communication systems," *IEEE Photon. J.*, vol. 7, no. 5, Oct. 2015, Art. no. 7904307.
[14] M. Asseri, *OFDM PAPR Reduction in SISO and MIMO Systems: The Mathematical Definitions and Analytical Methods*. Riga, Latvia: VDM Verlag Dr. Müller, 2011.
[15] S. H. Han and J. H. Lee, "An overview of peak-to-average power ratio reduction techniques for multicarrier transmission," *IEEE Wireless Commun.*, vol. 12, no. 2, pp. 56–65, Apr. 2005.
[16] M. Al-Rayif, "Partially orthogonal SLM in SISO OFDM system without side information," *Int. J. Res. Wireless Syst.*, vol. 2, no. 1, pp. 14–20, Mar. 2013.
[17] Y.-J. Cho, K.-H. Kim, J.-Y. Woo, K.-S. Lee, J.-S. No, and D.-J. Shin, "Low-complexity PTS schemes using dominant time-domain samples in OFDM systems," *IEEE Trans. Broadcast.*, vol. 63, no. 2, pp. 440–445, Jun. 2017.
[18] J.-Y. Woo, H. S. Joo, K.-H. Kim, J.-S. No, and D.-J. Shin, "PAPR analysis of class-III SLM scheme based on variance of correlation of alternative OFDM signal sequences," *IEEE Commun. Lett.*, vol. 19, no. 6, pp. 989–992, Jun. 2015.
[19] M. A. Khan and R. K. Rao, "Low-complexity PAPR reduction technique for OFDM systems using biased subcarriers," *Can. J. Elect. Comput. Eng.*, vol. 39, no. 1, pp. 19–25, 2016.
[20] K.-H. Kim, "On the shift value set of cyclic shifted sequences for PAPR reduction in OFDM systems," *IEEE Trans. Broadcast.*, vol. 62, no. 2, pp. 496–500, Jun. 2016.
[21] VPIsystems™, "VPItransmissionMaker™," http://www.vpiphotonics.com/index.php. Accessed: November 25, 2018.
[22] R. F. Fischer and M. Hoch, "Peak-to-average power ratio reduction in mimo OFDM," in *Proc. Int. Conf. Commun.*, 2007, pp. 762–767.
[23] M. Al-Rayif, H. Seleem, A. Ragheb, and S. Alshebeili, "Experimental demonstration for PAPR reduction in OFDM system using partial-OSLM technique," *J. Circuits, Syst. Comput.*, vol. 27, no. 7, 2018, Art. no. 1850106.
[24] C. Rapp, "Effects of HPA-nonlinearity on a 4-DPSK/OFDM-signal for a digital sound broadcasting signal," in *Proc. ESA, 2nd Eur. Conf. Satell. Commun.*, 1991, pp. 179–184 (SEE N92-15210 06-32).